**RESEARCH**

# Impact of contrast-enhanced CT in the dosimetry of SBRT for liver metastases treated with MR-Linac

Min Liu[1,2,3], Mingzhe Liu[1,4*] , Feng Yang[2,3] , Yanhua Liu[1], Shoulong Wang[2,3], Yazhen Chen[5], Jie Li[2,3], Xianliang Wang[2,3] and Lucia Clara Orlandini[2,3]

## Abstract

**Background** To investigate the impact of using contrast-enhanced computed tomography (CHCT) in the dosimetry of stereotactic body radiation therapy (SBRT) for liver metastases treated with MR-Linac.

**Methods** A retrospective study was conducted on 21 liver cancer patients treated with SBRT (50 Gy in 5 fractions) using a 1.5 Tesla Unity MR-Linac. The clinical treatment plans optimised on plain computed tomography (pCT) were used as reference. The electronic density (ED) of regions of interest (ROIs) including the liver, duodenum, esophagus, spinal cord, heart, ribs, and lungs, from pCT and CHCT, was analysed. The average ED of each ROI from CHCT was used to generate synthetic CT (sCT) images by assigning the average ED value from the CHCT to the pCT. Clinical plans were recalculated on sCT images. Dosimetric comparisons between the original treatment plan ($TP_{pCT}$) and the sCT plan ($TP_{sCT}$) were performed using dose-volume histogram (DVH) parameters, and gamma analysis.

**Results** Significant ED differences ($p < 0.05$) were observed in the liver, great vessels, heart, lungs, and spinal cord between CHCT and pCT, with the lungs showing the largest differences (average deviation of 11.73% and 12.15% for the left and right lung, respectively). The target volume covered by the prescribed dose ($V_{Dpre}$), and the dose received by 2% and 98% of the volume ($D_{2\%}$, and $D_{98\%}$, respectively) showed statistical differences ($p < 0.05$), while the gradient index (GI) and the conformity index (CI) did not. Average deviations in target volume dosimetric parameters were below 1.02%, with a maximum deviation of 5.57% for. For the organs at risk (OARs), significant differences ($p < 0.05$) were observed for $D_{0.35cc}$ and $D_{1.2cc}$ of the spinal cord, $D_{10cc}$ for the stomach, $D_{0.5cc}$ for the heart, and $D_{30\%}$ for the liver-GTV, with mean deviations lower than 1.83% for all the above OARs. Gamma analysis using 2%-2 mm criteria yielded a median value of 95.64% (range 82.22–99.65%) for the target volume and 99.40% (range 58–100%) for the OARs.

**Conclusion** The findings suggest that the use of CHCT in the SBRT workflow for liver metastases may result in minor target volume overdosage, indicating its potential for adoption in clinical settings. However, its use should be further explored in a broader context and tied to personalized treatment approaches.

**Keywords** MR-Linac, Contrast media, Liver cancer, SBRT, Synthetic CT, MR guided adaptive radiotherapy

Feng Yang Co-first author.

*Correspondence:
Mingzhe Liu
liumz@cdut.edu.cn

Full list of author information is available at the end of the article

Liu *et al. Radiation Oncology*     (2024) 19:144

Page 2 of 10

## Background

Contrast media (CM) improve the contrast resolution of imaging modalities by differentiating soft-tissue densities and are widely used in radiology, cardiology, gastrointestinal and vascular surgery, and urology procedures. In radiotherapy, CM may be used during the acquisition of computed tomography (CT) or magnetic resonance (MR) images to assist physicians in identification and delineation of targets and organs at risk (OARs) [1, 2]. Nevertheless, a significant concern with its use in the planning CT is related to the increased attenuation due to the CM, which may affect dose calculations. Whether the use of CM can affect the dose calculation of radiation therapy has been reported in the literature for several treatment sites. Yuta Shibamoto et al. showed that in whole brain, mediastinum, and whole pelvic irradiation, the increase in monitor units (MU) caused by CT CM was less than 1% and the effect was negligible. But for upper abdominal tumors, MU increased by more than 2% [3]. Jianghong Xiao et al. demonstrated that in lung cancer radiotherapy, the use of CM affects Hounsfield Units (HU) but has a minimal and clinically permissible impact on the radiotherapy dose, regardless of the technology used [4]. Hee Jung Kim et al. investigated the effect of CM on dose calculations in CyberKnife radiotherapy for different tumor sites; they found that while the average dose deviation caused by the CM is less than 2%, this deviation can increase significantly to 7.8% depending on the target location. In Jianping Zhang et al.'s study, patients treated with CyberKnife brain stereotactic radiosurgery (SRS) were categorized based on the target area's tissue homogeneity. Dose deviation and gamma non-pass rates were higher in heterogeneous tissue areas compared to homogeneous ones. Thus they recommend to use plain CT (pCT) for planning target areas sensitive to CM and near heterogeneous tissues [5]. This highlights the importance of considering the impact of CM in treatment planning to ensure accurate dose delivery [6].

MR-guided adaptive radiotherapy (MRgART) has seen a significant surge with the availability of the MR-Linac [7, 8]. MR-Linac systems are distinguished by their capacity to acquire MR imaging during each treatment session, offering superior soft tissue differentiation compared to conventional imaging modalities such as cone-beam CT (CBCT) and CT scans [9, 10] used for image guided radiotherapy (IGRT). This enhanced imaging capability, combined with the ability to reoptimize treatments online, positions MR-Linac at the forefront of radiotherapy innovation [11]. These advancements facilitate highly precise and adaptive radiotherapy, leading to significant improvements of the related clinical research [11–13].

The Unity MR-Linac combine a 1.5T MR scanner and a 7MV linear accelerator and has been increasingly used for stereotactic body radiation therapy (SBRT) in liver cancer to better tumor targeting and sparing of healthy tissues. William A. HalI et al. were the first to use Unity to perform SBRT on liver metastases, primary liver cancer, and pancreatic cancers; their study demonstrated that patients tolerated the entire treatment process well, with no significant radiotoxicity observed post treatment [14]. Michael Mayinger et al. 's study showed that online adaptive planning of SBRT for liver cancer patients based on MR-Linac can effectively improve the dose coverage of tumors [15]. van de Lindt T N et al. successfully performed 4D- magnetic resonance imaging (MRI)-guided SBRT therapy for liver cancer in a MR-Linac [16].

Adapted plans based on the daily MRI require the assignment of a relative electron density (ED) map to allow for accurate dose calculation. At Unity MR-Linac when calculating MR-based synthetic CT (sCT) plans, the strategy is to use bulk density assignment based on the contours drawn on the original patient simulation CT; sCT images are generated using the average relative ED from the CT reference plan, allowing for dose calculations on the MR images [17]. ED is derived from the CT Hounsfield Units (HU), making HU a crucial parameter in radiotherapy treatment planning. HU values are influenced by factors such as CT acquisition settings, scanner model, and material density. Moreover, variation in respiratory states during image acquisition – such as free breathing, breath hold, etc..- can affect tissue density, thereby impacting HU, ED and ultimately the dose accuracy [18, 19]. The presence of CM in the reference CT can affect HU, which are related to relative ED [5]. As for other treatment sites, the impact of CM on dose distribution in liver cancer patients remains uncertain. Xiao et al. have determined that the use of CM introduces dose deviations in SBRT for hepatocellular carcinoma [20]. Kamal R et al. suggested that dose calculation can be performed on contrast-enhanced CT (CHCT) images when overriding heart electron densities for liver cancer SBRT [21]. Contradictions exist between studies, and even minor dose changes during SBRT may risk surrounding organs. Although several studies highlight that CM improve liver lesions visibility and aid treatment planning [22], the impact on dose calculation using CHCT remains to be deeply explored.

This study investigates for a cohort of patients treated with MRgART at Unity the potential differences in plan dosimetry that can arise if CHCT is used as a reference for the treatment plan, providing valuable insights for clinical practice.

## Methods

### Patients

This retrospective study included 21 patients admitted to Sichuan Cancer Hospital between August and December

2023 to undergo SBRT for liver metastases at MR-Linac. Patient characteristics and treatment details are summarized in Table 1. Figure 1 provides a representative 3D image showing the location of the liver metastases analysed and surrounding OARs. Written informed consent was obtained from all patients, and the study was approved by the hospital Institutional Ethics Committee (SCCHEC-02-2024-078).

### Imaging acquisition at simulation CT

Patients were set up in the supine position using indexed positioning aids and were immobilized with a vacuum pillow (BlueBAG, Elekta AB, Stockholm, Sweden). A few days before the start of the treatment, patients underwent a 4-dimensional computed tomography (4DCT) scan with Brilliance big bore scanner (Philips Medical System, Cleveland, OH, USA); a first non-contrast CT scan used for the treatment planning was acquired, followed by one with the CM, used to support the physician in tumor delineation. For the CHCT scan, patients were injected intravenously on the right arm with iodixanol with an iodine concentration of 37 g/100 ml or 32 g/100 ml, if over or under the age of 63, respectively; the injection rate was 2.0 ml/s, and the total injection amount was 1.5 times of the patient's body weight in kg. The CHCT was acquired 60 s after the injection of the CM during the portal venous phase, following internal protocol guidelines, to allow for optimal visualization of the liver's

**Table 1** Patients and treatment characteristics

| Patients | |
|---|---|
| Number | 21 |
| Years, median (range) | 52.5 (29–73) |
| Weight (kg), median (range) | 61.0 (36–84) |
| Female - no. (%) | 12 (57.1%) |
| Male - no. (%) | 9 (42.9%) |
| **[a]PTV – no. (%)** | |
| 4 cc < Volume < 14 cc | 7 (33.3%) |
| 14 cc < Volume < 24 cc | 5 (23.8%) |
| 24 cc < Volume < 34 cc | 3 (14.3%) |
| 34 cc < Volume < 54 cc | 6 (28.6%) |
| Volume(cc), median (range) | 27.9 (9.8–71.4) |
| **Closest[b]OARs – no. (%)** | |
| Duodenum | 0(0%) |
| Esophagus | 2 (9.5%) |
| Great Vessels | 1 (4.8%) |
| Heart | 4 (19.0%) |
| Liver -[c]GTV | 2 (9.5%) |
| Spinal cord | 2 (9.5%) |
| Rib | 8 (38.1%) |
| Stomach | 3(14.3%) |
| Small Bowel | 4(19.0%) |
| Lung | 5(23.8%) |
| Kidney | 1(4.8%) |

[a]PTV: planning target volume; [b]OARs: organ at risk; [c]GTV: gross target volume

vasculature and parenchyma [23, 24]. The 4DCT was acquired to obtain the CT images of the patient at different breathing phases.

CT and CHCT imaging were exported into a segmentation commercial software (PVmed Contouring Software, Guangzhou, China) for the automatic segmentation of all the regions of interest (ROIs) [25]; the delineated ROIs and images were exported into a commercial software (MIM Software Inc, Cleveland Ohio, USA) where experienced radiation oncologists delineated the target and validate/modify the OARs automatically segmented.

### Reference treatment plan

Target and OARs contouring was performed following the Stereotactic Ablative Radiation Therapy (SABR) UK consortium guidelines [26]. Patients were treated in an SBRT regimen at Unity 1.5 Tesla MR-linac (Elekta Unity, Elekta AB, Stockholm, Sweden) and were scheduled to receive a prescription dose of 50 Gy in 5 fractions. Monaco Version 5.4 (Elekta AB, Stockholm, Sweden) treatment planning system (TPS) was used for the plan optimization to achieve the clinical goals, particularly to cover at least 95% of the target volume with the dose prescribed, the maximum dose falling within the range of 110–140% of the dose prescribed while keeping the OARs doses as low as possible following the international guidelines and consensus [27]; OARs constraints and target goals used for plan optimization and validation are shown in Table 2, with the added indication that in case of a conflict between the target coverage and the OAR limits, the target will be compromised. The CT reference plans were optimised on the pCT using 9 to 11 individual beam angles, excluding angles between 110° and 135° and 230° to 255° to avoid the high-density areas of the couch, and 0° to 30° to avoid the magnetic coil [28]; a 2 mm dose grid and a 1% uncertainty per calculation were used. The reference CT plan contains all the density bulk assignment information i.e., the contours, their corresponding average ED and the priority of each contour concerning density assignment in case of contour overlaps. These information are crucial during the online adaptive step, where MRI-based sCT images are used for recalculating the adaptive plan [29].

### Online adaptive radiotherapy

Each treatment fraction starts with the acquisition of a first online MRI to use for the plan adaptation. The reference CT (or the MRI scan of a previous session), contours and plan, together with the daily online MRI are used as input to adapt the plan for that specific session. The MRI or CT scan used as reference is matched with the online MRI through rigid registration, and the isocenter position in the reference data is updated; then the workflow may proceed with an adapt to shape (ATS) or adapt to
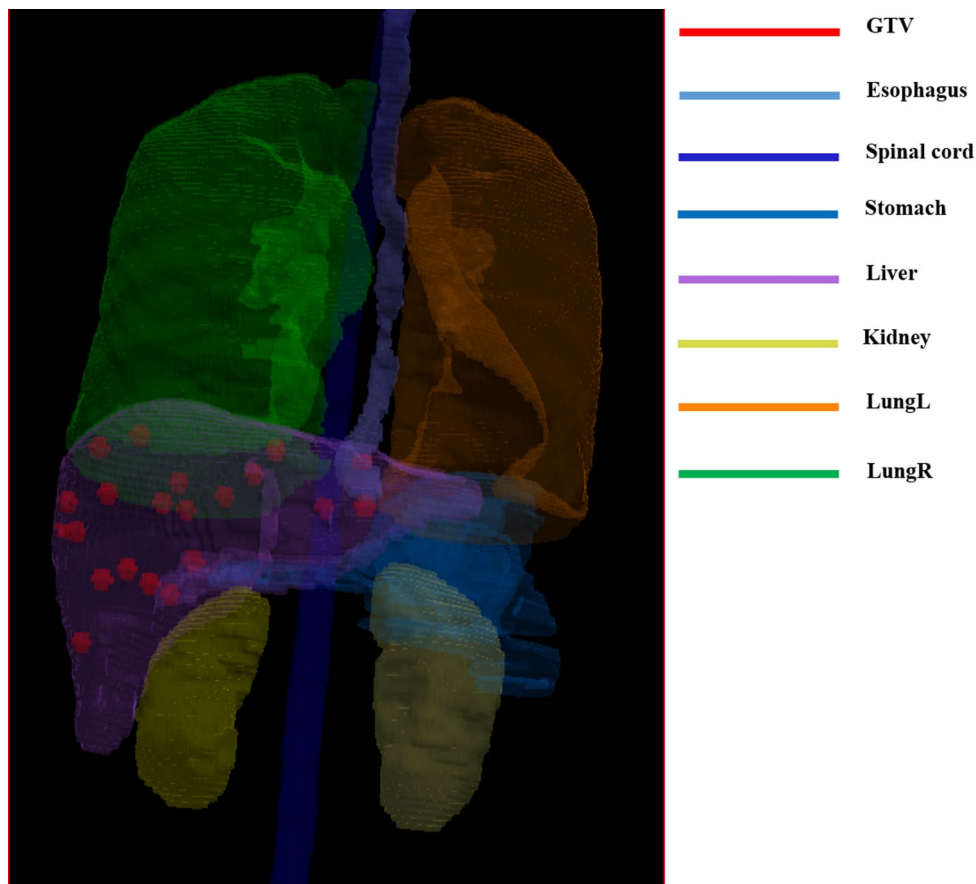
**Fig. 1** 3D representative image showing the location of the liver metastases included in the study

position (ATP) approach; the ATS is needed when the OARs and/or the targets do not match with the daily patient anatomy; in this case the adapted plan is reoptimized on the daily MR-based sCT [17, 30]. The strategy of sCT applied in Monaco TPS is to assigning average ED based on the contours drawn on patient simulation CT. More specifically, the daily acquired MRI will be deformably registered to simulation CT, then all contours information including average ED and the priority of density assignment on CT are propagated to MRI to generate the sCT. In the ATP approach after the rigid registration of the online MRI and the reference CT images, the plan is reoptimised directly on the reference CT without any change on the ROIs contouring. In both workflows, a second MRI is acquired in real time during the delivery [31]. Figure 2 shows the flowchart of the online procedure for MR-based adaptive radiotherapy at Unity MR-Linac.

**Use of CHCT for sCT generation and plan recalculation**

For each patient the consistency of the respiratory phase between the CT and the corresponding CHCT scan [18] was assessed by the radiation oncologist to avoid variations in ED not strictly related to the use of CM. CHCT images and the corresponding ROIs delineated by Pvmed

software were imported into the Monaco TPS to assess the average ED of each structure, including the OARs. For each patient, a sCT was generated assigning for each of the ROI delineated on pCT the average ED assessed on the CHCT. In Fig. 3, CT, CHCT and corresponding generated sCT transversal images of a representative patient are shown. The sCT treatment plan ($\text{TP}_{\text{sCT}}$) was obtained recalculating the reference treatment plan on using the corresponding sCT image without altering any of the plan parameters.

**sCT and pCT plan comparison**

Target and OARs dose volume histogram (DVH) dosimetric differences between $\text{TP}_{\text{pCT}}$ and $\text{TP}_{\text{sCT}}$ were assessed. The target volume receiving 100% of the prescribed dose ($\text{V}_{\text{Dpre}}$), the dose received by 2% and 98% of the volume ($\text{D}_{2\%}$, $\text{D}_{98\%}$, respectively), the max and minimum points dose ($\text{D}_{\text{max}}$, $\text{D}_{\text{min}}$, respectively) were used; additionally, the conformity index (CI), and the gradient index (GI) were evaluated. The CI is defined as the ratio of the volume encompassed by the prescription dose to the planning target volume (PTV) [32]. The GI is described as the ratio of the volume receiving 50% of the prescription dose ($\text{V}_{50\%}$) to the PTV volume [33].

Liu *et al. Radiation Oncology*    (2024) 19:144

Page 5 of 10

**Table 2** OARs constraints and target goals in SBRT for liver metastasis receiving 50 gy in 5 fractions

| Region of interest | Criteria | Region of interest | Criteria |
|---|---|---|---|
| [a]PTV | | Stomach | |
| [b]$V_{100\%(50Gy)}$ | ≥ 95% | [c]$D_{max\,(0.5cc)}$ | < 32 Gy |
| [b]$V_{95\%}$ (47.5Gy) | ≥ 99% | c$D_{10cc}$ | < 18 Gy |
| [c]$D_{max\,(0.5cc)}$ | (110%∼140%)$D_{pre}$; (55 Gy ∼ 70 Gy) | Rib | |
| [d]$D_{min}$ | ≥ 90%$D_{pre}$(45 Gy) | [c]$D_{max}$ | < 43 Gy |
| Liver minus GTV | | [c]$D_{1cc}$ | < 35 Gy |
| [e]$D_{700cc}$ | $^<$18 Gy | Kidney | |
| [f]$D_{30\%}$ | < 18 Gy | [g]$V_{10Gy}$ | < 10% |
| Spinal cord | | [h]$D_{mean}$ | < 10 Gy |
| [c]$D_{max}$ | < 30 Gy | Small bowel | |
| [e]$D_{0.35cc}$ | < 23 Gy | [c]$D_{max\,(0.5cc)}$ | < 30 Gy |
| [e]$D_{1.2cc}$ | < 14 Gy | [e]$D_{15cc}$ | < 19.5 Gy |
| Heart | | Duodenum | |
| [c]$D_{0.5cc}$ | < 27 Gy | [c]$D_{5cc}$ | < 18 Gy |
| Lung right and left | | [c]$D_{10cc}$ | < 12 Gy |
| [e]$D_{1000cc}$ | < 13.5 Gy | Esophagus | |
| [e]$D_{1500cc}$ | < 12.5 Gy | [c]$D_{5cc}$ | < 19.5 Gy |

[a]PTV: planning target volume; $V_{x\%}$: volume covered by x% of the prescription dose; [c]$D_{max}$: maximum dose [d]$D_{min}$: minimum dose; [e]$D_{y\,cc}$: dose received y cube centimetres; [f]$D_{z\%}$: dose received z% of the volume; [g]$V_{u}$: volume covered by U dose; [h]$D_{mean}$: mean dose

For the OARs the dose received by x cube centimeters or x% of the volume ($D_{xcc}$, $D_{x\%}$), and $D_{max}$ were used. For $V_{Dpre}$ the comparison was performed by the percentage point subtracting the value of the dosimetric parameter of $TP_{sCT}$ from the corresponding values of $TP_{pCT}$, whilst for the dosimetric parameter expressed in Gy, the percentage dose difference was considered.

Target and OARs dose distributions were assessed using gamma analysis with 2%-2 mm criteria and lower dose threshold of 5% of the prescription dose, using CERR v4.4 (https://github.com/cerr/CERR).

Following internal guidelines that strive to keep the overall dosimetric discrepancy of the treatment as low as possible, the sCT treatment plan recalculated from the reference CT plan is considered in agreement when $\gamma < 1$ is higher than 99% with the criteria and the target dose difference at any point of the DVH is lower than 1.5% or 1 Gy, as also reported in a previous study from our group [17].

Statistical analysis of the data was performed by using SPSS software (IBM, Armont, USA) version 25.0, used to test the results of the dosimetric parameters of the $TP_{sCT}$ and $TP_{pCT}$ by paired t-test or Wilcoxon rank-sum depending on the result of the normality test; a *p* value *p*<0.05 was considered statistically significant.

## Results

The ED assessed for a total of 42 imaging datasets (CT and corresponding CHCT) of 21 patients who underwent liver metastases SBRT treatment at Unity MR-Linac were compared. The mean ED for each structure (body, liver, heart, lungs, spinal cord, duodenum, great vessels, ribs, esophagus, small bowel, etc.) calculated on CT and CHCT based on the average ED values obtained from the patient cohort are reported in Table 3 along with their comparison. The ED for various tissues, as reported in the international standards for radiation therapy and radiological protection ICRU Report 46 [34] and ICRP 110 [35], are also listed as reference; these ED are relative values, determined by the ratio of the tissue's absolute ED to that of water. For the lungs, imaging datasets from three patients were excluded because the scans did not cover the entire lung volume due to the target's location
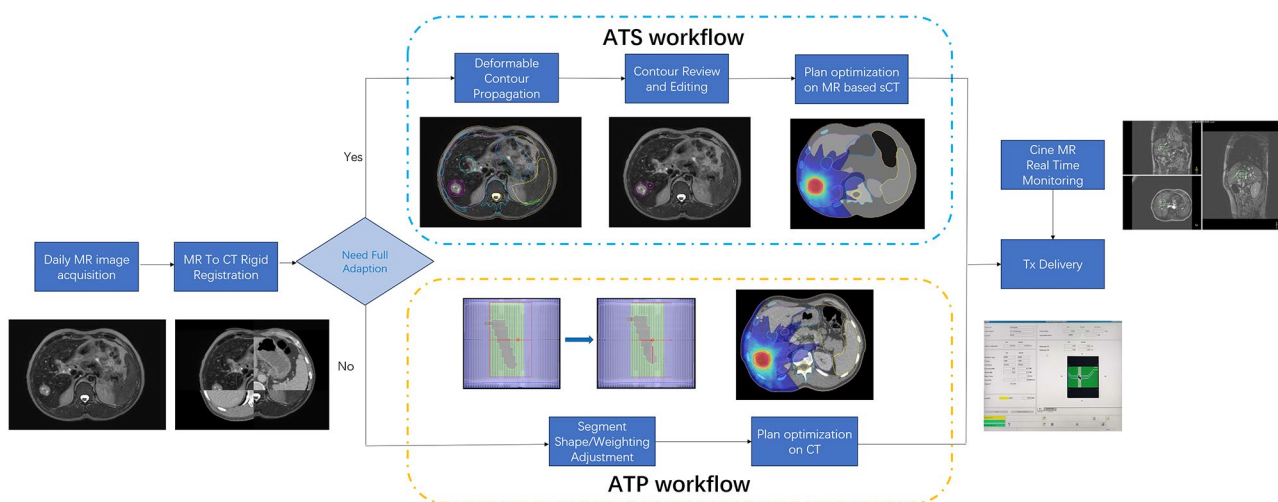


**Fig. 2** Flowchart of the online adaptive radiotherapy process at Unity MR-Linac
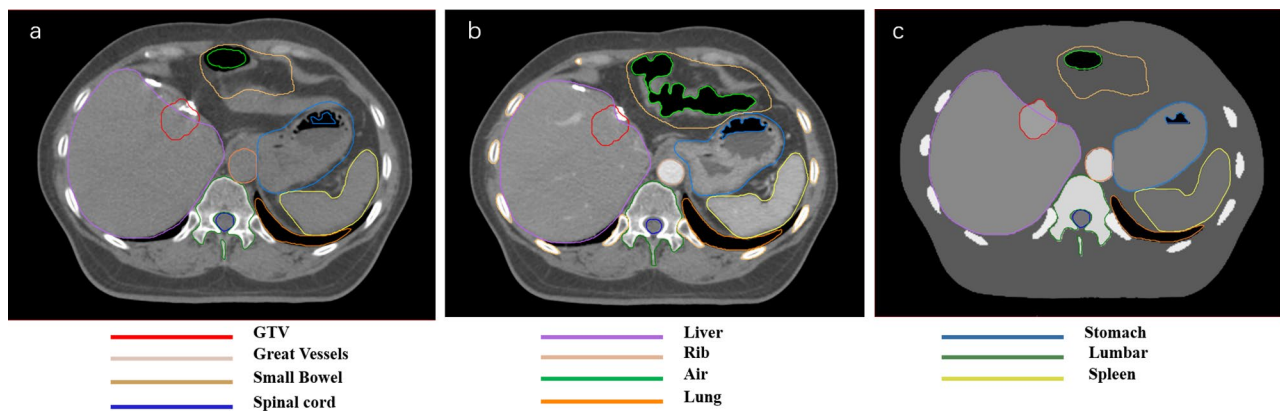
| GTV | Liver | Stomach |
| Great Vessels | Rib | Lumbar |
| Small Bowel | Air | Spleen |
| Spinal cord | Lung | |

**Fig. 3** Synthetic CT (**c**) obtained from the plain CT (**a**) and contrast-enhanced CT (**b**) in transversal images for a representative patient

**Table 3** Electrons density (ED) values for regions of interest (ROIs) assessed on plain CT and contrast-enhanced CT (CHCT) and their comparison

| ROIs | No. of patients | Ref** | pCT Mean ± SD | CHCT Mean ± SD | pCT vs. CHCT Max Diff (%) | pCT vs. CHCT Mean (%) ± SD | p |
|---|---|---|---|---|---|---|---|
| Liver-GTV | 21 | 1.05 | 1.06 ± 0.01 | 1.09 ± 0.01 | 3.93 | 2.42 ± 0.78 | <0.001* |
| Spinal Cord | 21 | 1.04 | 1.04 ± 0.00 | 1.04 ± 0.01 | 0.77 | 0.31 ± 0.2 | <0.001* |
| Heart | 21 | 1.04 | 1.03 ± 0.01 | 1.09 ± 0.01 | 9.03 | 6.18 ± 1.27 | <0.001* |
| Great Vessels | 21 | 1.06 | 1.05 ± 0.00 | 1.14 ± 0.02 | 11.48 | 8.35 ± 1.61 | <0.001* |
| Rib | 21 | 1.44 | 1.2 ± 0.04 | 1.21 ± 0.04 | 4.73 | 0.5 ± 1.19 | 0.069 |
| Left Lung^ | 18 | 0.26 | 0.31 ± 0.06 | 0.34 ± 0.06 | 21.05 | 11.73 ± 5.46 | <0.001* |
| Right Lung^ | 18 | 0.26 | 0.29 ± 0.06 | 0.33 ± 0.06 | 18.15 | 12.15 ± 5.41 | <0.001* |
| Tissue | 21 | 1.02 | 0.95 ± 0.04 | 0.97 ± 0.04 | 4.78 | 2.21 ± 1.41 | <0.001* |
| Esophagus | 21 | 1.04 | 1.02 ± 0.03 | 1.03 ± 0.03 | 3.41 | 1.52 ± 1.09 | <0.001* |
| Duodenum | 21 | 1.02 | 1.03 ± 0.02 | 1.06 ± 0.02 | 5.47 | 3.46 ± 1.38 | <0.001* |
| Lumbar | 21 | 1.44 | 1.17 ± 0.02 | 1.18 ± 0.02 | 0.85 | 0.41 ± 0.23 | <0.001* |
| Small bowel | 21 | 1.02 | 0.99 ± 0.02 | 1.01 ± 0.03 | 3.09 | 1.67 ± 0.91 | <0.001* |
| KidneyL | 21 | 1.04 | 1.03 ± 0.01 | 1.1 ± 0.01 | 8.40 | 6.57 ± 0.91 | <0.001* |
| KidneyR | 21 | 1.04 | 1.03 ± 0.01 | 1.1 ± 0.01 | 8.59 | 6.57 ± 1.13 | <0.001* |
| Stomach | 21 | 1.02 | 1.02 ± 0.03 | 1.05 ± 0.02 | 9.97 | 2.47 ± 2.06 | <0.001* |

*Note* *$p < 0.05$ indicating significant difference; ** values from reference standards for radiation therapy and radiological protection (ICRU 46, ICRP 110)

^ scans from 3 patients were excluded because the imaging did not cover the entire lung volume, and because of the large difference on the acquisition phases of the pCT and the CHCT scans

near the lower lobe of the liver, and because of significant differences in the acquisition phases between the pCT and CHCT scans [36]. The average ED obtained on the pCT and CHCT for each of the structure shows significant differences ($p < 0.05$) with the larger deviations registered for the lungs (11.73% and 12.15% for the left and right lung respectively), great vessels (8.35%), and heart (6.18%). The ED values suggested by ICRU 46 correspond to those obtained from pCT; a discrepancy exists in the value for the ribs and the lumbar region from the different way of delineation used [37].

Of the 21 $TP_{pCT}$ delivered plans, 16 met the clinical requirements for both target coverage and OARs constraints, while for 5 patients, due to the proximity of the target with the ribs (4 patients) and stomach (1 patients), a lower target coverage ($81\% < V_{Dpre} < 91\%$) was accepted in order to meet the OARs constraints;

for the corresponding $TP_{sCT}$ the results show a variation of $V_{Dpre}$ with an median value of 0.83% (range 0.15 -2.03%), reducing the patients achieving the target goal ($V_{Dpre} > 95\%$) to 2 patients; moreover significant differences ($p < 0.05$) were found for the target $V_{Dpre}$, CI, $D_{2\%}$, $D_{98\%}$ of $TP_{pCT}$ and $TP_{sCT}$. Nevertheless, the deviation of $V_{Dpre}$ between $TP_{sCT}$ and $TP_{pCT}$ is higher than 1.5% for only 2 out of 21 patients (9.5%).

With regard to OARs, their position respect to the target, with the exception of the 5 patients where the target was close to the rib/stomach, was far enough away not to affect their dosimetry, resulting in doses well below the limits indicated by international guideline. Therefore, even though significant differences ($p < 0.05$) were found between $TP_{sCT}$ and $TP_{pCT}$ for the liver-GT $D_{30\%}$, spinal cord $D_{0.35cc}$ and $D_{1.2cc}$, heart $D_{0.5cc}$, and stomach $D_{10cc}$, the

doses received remain so far from the limits that these discrepancies are not clinically appreciable.

The OARs and target dosimetric parameters obtained with $TP_{pCT}$ and $TP_{sCT}$ are shown in Table 4; Fig. 4; for each patient studied, the left lung and the right lung and duodenum received doses below 2.5 Gy ($5\%D_{pre}$) in both treatment plans compared and have not been included.

The differences in dose distribution of $TP_{sCT}$ vs. $TP_{pCT}$ assessed with the global gamma analysis for the heart, stomach, liver-GTV and target, confirm the discrepancies found using the comparison of the DVH dosimetric parameters and the statistical analysis. For the target the pass rate range between 82.22% and 99.65%, for the heart between 58.00% and 100.0%, and for the stomach between 95.0% and 100%, while the gamma analysis for the spinal cord and the liver minus GTV do not highlight discrepancies. The details of the gamma analysis are shown in the Table 5.

## Discussion

CM are widely used in radiation therapy during the simulation CT to improve the delineation of tumor volume and OARs. However, the use of CHCT images as a reference for treatment planning may lead to dosimetric

discrepancies due to difference in ED values of various structures [3–6]. During MRgART at unity MR-linac the daily adaptive plans are performed on MR-based sCT using the ATS workflow, or on reference CT or MRI when using the ATP workflow. In both cases, the ED values from the reference CT are used in the daily plan calculation. It is therefore crucial to determine whether CHCT can be reliably used as reference CT images.

According to the results of this study, the average ED of OARs such as liver, great vessels, heart, and lungs differ significantly from those obtained with pCT. This disparity arises because the contrast agent is administered intravenously and travels through the bloodstream, leading to higher concentrations in these organs. The liver also accumulates contrast due to its role in filtering blood, but the ribs, spinal cord, and other tissues are less affected. However, when comparing the dosimetry of liver SBRT between $TP_{sCT}$ and $TP_{sCT}$, the impact on plan dosimetry was evident in only 2 out of 21 patients (less than 10%). The higher discrepancies in the target dosimetric parameter were 2.03% for $V_{Dpre}$ and 5.57% for $D_{min}$, with average differences lower than 2%, also for OARs dosimetry. The impact on plan dosimetry on the use CHCT as a reference scan, remains therefore minimal for the cohort

**Table 4** Comparison of $TP_{pCT}$ and $TP_{sCT}$ DVH dosimetric parameters; median values and in parenthesis minimum and maximum; *p* values in bold represent a significant difference

|  | N° | Parameter | $TP_{pCT}$ | $TP_{sCT}$ | Difference (%) | *p* |
|---|---|---|---|---|---|---|
| PTV | 21 | [a]$V_{Dpre}$(Gy) | 93.2(81.00~95.11) | 92.56(80.24~95.94) | 0.83(0.15~2.03) | **<0.001** |
|  | 21 | [b]$D_{2\%}$(Gy) | 66.75(62.26~68.91) | 66.55(61.55~68.75) | 0.52(0.01~1.37) | **0.035** |
|  | 21 | [b]$D_{98\%}$(Gy) | 46.32(36.46~48.79) | 46.06(36.30~48.91) | 0.73(0.18~1.44) | **<0.001** |
|  | 21 | [c]$D_{max}$(Gy) | 68.18(63.50~70.87) | 68.01(62.38~71.23) | 0.58(0.02~1.76) | 0.136 |
|  | 21 | [d]$D_{min}$(Gy) | 39.40(27.39~45.74) | 39.23(27.48~46.00) | 1.02(0.07~5.57) | 0.253 |
|  | 21 | [e]CI | 0.83(0.71~0.92) | 0.82(0.71~0.91) | 0.54(0.00~2.71) | 0.055 |
|  | 21 | [f]GI | 3.97(3.27~4.95) | 3.99(3.24~4.86) | 0.97(0.16~2.15) | 0.051 |
| Liver-GTV | 5 | [g]$D_{700cc}$(Gy) | 5.81(2.90~9.38) | 5.78(2.89~9.33) | 0.73(0.01~3.27) | * |
|  | 14 | [b]$D_{30\%}$(Gy) | 8.04(3.94~15.09) | 7.99(3.92~15.01) | 0.67(0.12~1.65) | **<0.001** |
| Spinal Cord | 18 | [c]$D_{max}$(Gy) | 8.58(3.81~15.22) | 8.59(3.89~15.62) | 1.29(0.16~3.16) | 0.689 |
|  | 15 | [g]$D_{0.35cc}$(Gy) | 8.36(2.84~14.44) | 8.33(2.90~14.41) | 0.8(0.14~2.28) | **0.044** |
|  | 14 | [g]$D_{1.2cc}$(Gy) | 7.53(3.95~13.32) | 7.47(3.89~13.36) | 1.08(0.18~2.34) | **0.002** |
| Heart | 13 | [c]$D_{max}$(Gy) | 13.06(3.47~35.22) | 12.90(3.54~34.75) | 1.32(0.28~2.69) | 0.056 |
|  | 13 | [g]$D_{0.5cc}$(Gy) | 11.28(2.98~29.82) | 11.11(3.00~29.11) | 1.35(0.11~5.45) | **0.039** |
| Esophagus | 6 | [g]$D_{5cc}$(Gy) | 6.15(2.83~12.32) | 6.13(2.84~12.35) | 0.63(0.07~1.43) | * |
| Stomach | 20 | [c]$D_{max}$(Gy) | 12.12(3.67~29.84) | 12.04(3.49~29.42) | 1.59(0.04~4.95) | 0.091 |
|  | 16 | [g]$D_{10cc}$(Gy) | 8.93(4.07~16.29) | 8.87(4.01~16.37) | 0.98(0.10~1.77) | **0.024** |
| Rib | 21 | [c]$D_{max}$(Gy) | 28.71(15.24~40.95) | 28.68(15.42~41.25) | 1.23(0.05~4.82) | 0.665 |
|  | 21 | [g]$D_{1cc}$(Gy) | 23.14(12.47~34.82) | 23.08(12.56~34.85) | 0.66(0.08~4.04) | 0.194 |
| Small Bowel | 13 | [c]$D_{max}$(Gy) | 15.07(4.01~28.06) | 15.02(3.93~27.33) | 1.83(0.43~4.35) | 0.582 |
|  | 10 | [g]$D_{5cc}$(Gy) | 10.58(3.00~18.29) | 10.57(2.94~18.52) | 1.04(0.16~2.15) | 0.990 |

[a]$V_{Dpre}$, volume covered by the prescription dose; [b]$D_{z\%}$, dose received z% of the volume; [c]$D_{max}$, point of maximum dose; [d]$D_{min}$, minimum dose; [e]CI, conformity index; [f]GI, gradient index, [g]$D_{ycc}$: dose received y cube centimeters; *statistical analysis was not performed due to the small number of patients

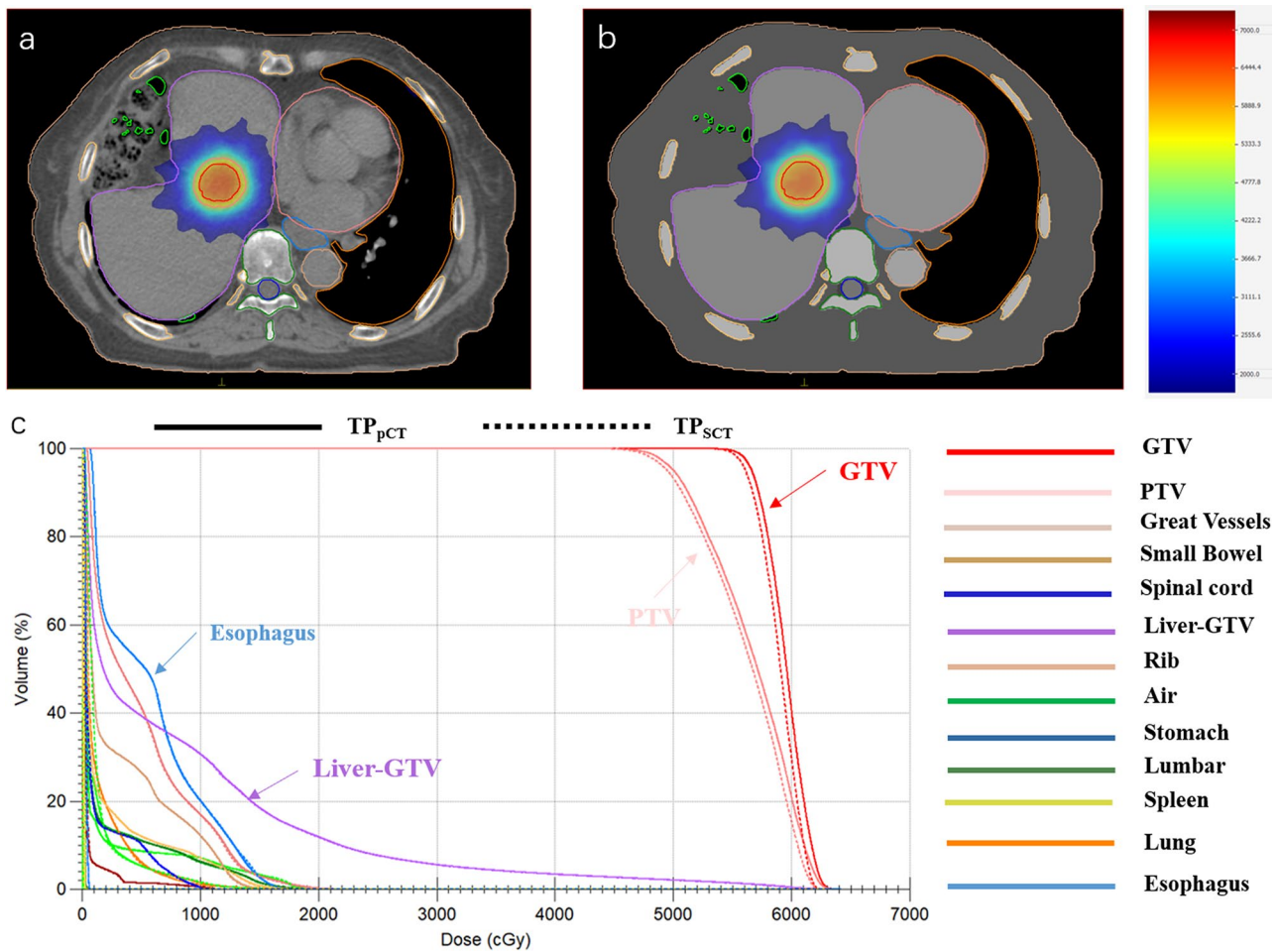*Note* dose lower than 2.50 Gy were not considered in the analysis

Liu *et al. Radiation Oncology*        (2024) 19:144

Page 8 of 10



**Fig. 4** Dose distribution in a pCT (**a**) and sCT (**b**) transversal image and DVH comparison for a representative patient

**Table 5** $TP_{sCT}$ vs. $TP_{pCT}$ target and OARs gamma analysis with 2%-2 mm criteria

| ROI | No. of cases | γ(2%-2 mm)% |
|---|---|---|
| PTV | 21 | 95.64 (82.22 ~ 99.65) |
| Liver-GTV | 21 | 99.71 (98.97 ~ 99.97) |
| Spinal Cord | 20 | 100.00 (100.00 ~ 100.00) |
| Heart | 13 | 96.69 (58.00 ~ 100.00) |
| Esophagus | 16 | 99.98 (99.96 ~ 100.00) |
| Stomach | 20 | 99.61 (95.00 ~ 100.00) |
| Rib | 21 | 99.87 (98.69 ~ 100.00) |
| Small bowel | 13 | 99.33 (94.53 ~ 100.00) |
| Body | 21 | 99.15 (95.53 ~ 99.96) |

*Note* organs with dose lower than 2.50 Gy were excluded from the analysis

of patients studied. The treatment plans were designed with the radiation predominantly passing through the liver, and the average difference caused by the contrast agent to the ED of the liver is only 2.42%, resulting in minimal impact on the target dose coverage. Nevertheless, the well-known risks associated with CM must be considered, including potential allergic reactions and increased costs in the management of the procedure. In liver patients, there is a particular concern for contrast-induced nephropathy, especially in those with comorbidities or preexisting renal issues. These risks make the routine use of CM in CBCT, MRI, and other modalities for image-guided radiotherapy challenging in vulnerable patient groups.

The research has several limitations. First, the relatively small patient cohort limits the statistical power and generalizability of the findings. Variations in imaging protocols and CM administration can introduce inconsistencies that affect data comparability; the timing between CM injection and CT acquisition can impact organ visibility and delineation by enhancing hypovascular lesions while potentially obscuring hypervascular tumors as they blend with the liver parenchyma. The single-institution setting further restricts the variability in patient demographics and tumor characteristics. Moreover, differences in the timing of CT acquisitions relative to the administration of CM can lead to discrepancies in ED, thereby impacting dose calculations. Additionally, both CT and CHCT scans were acquired during free breathing, which may result in different respiratory phases and

Liu *et al. Radiation Oncology*      (2024) 19:144

Page 9 of 10

non-synchronized scans, potentially causing slight image blurring [38] and introducing additional uncertainty in ED measurements [39]. However, since the study focuses on the liver region, where respiratory effects are less significant, and involves a relative comparison of CT and CHCT dosimetry, the impact of these factors is likely minimal.

Nevertheless, our findings underscore several important aspects. First, the use of CHCT leads to minimal dosimetric differences in the planning for liver SBRT. Second, the consistency in OAR dosimetry was generally maintained, with only minor dosimetric impact, suggesting that CHCT provides reliable information for OARs without compromising the accuracy of the treatment plan. Importantly, the limited influence of CM on dosimetric calculations indicates that CHCT does not significantly affect overall dose distribution. Additionally, it is noteworthy that the significant deviations found in the average ED of the lungs emphasize the potential for substantial dose deviations that may occur in lung SBRT. Future studies should consider larger, multi-institutional cohorts and the use of standardized imaging protocols to mitigate these limitations and provide more comprehensive insights into the role of CHCT in radiation therapy.

## Conclusion

CHCT in the SBRT workflow for liver metastases may lead to minor overdosage of the target volume in some patients, suggesting it could be considered for clinical adoption. However, its use should be investigated within a broader clinical framework and tailored to a personalised treatment strategy.

### Abbreviations

| | |
|---|---|
| CHCT | Contrast-enhanced computed tomography |
| SBRT | Stereotactic body radiation therapy |
| MR-Linac | Magnetic resonance linear accelerators |
| MU | Monitor units |
| ED | Electronic density |
| ROIs | Regions of interest |
| pCT | Plain CT |
| sCT | Synthetic computed tomography |
| DVH | Dose volume histogram |
| $TP_{pCT}$ | The original treatment plan |
| $TP_{sCT}$ | The sCT treatment plan |
| $V_{Dpre}$ | Target volume covered by the prescribed dose |
| CI | The conformity index |
| GI | The gradient index |
| OAR | Organs at risk |
| CM | Contrast media |
| IMRT | Intensity Modulated Radiation Therapy |
| 3D-CRT | 3-dimensional conformal radiation therapy |
| SRS | Stereotactic radiosurgery |
| MR | Magnetic resonance |
| ATS | Adapt to shape |
| ATP | Adapt to position |
| HU | Hounsfield units |
| 4D-CT | 4-dimensional computed tomography |
| MRI | Magnetic resonance imaging |
| MRgART | Magnetic resonance-guided adaptive radiotherapy |
| TPS | Treatment planning system |
| ICRU | The International Commission on Radiation Units and Measurements |
| ICRP | The International Commission on Radiological Protection |
| PTV | Planning target volume |
| CT | Computed tomography |
| GTV | Gross target volume |
| SABR | Stereotactic ablative radiation therapy |

## Declarations

### Ethics approval and consent to participate
The authors declare that this retrospective study "The effect of contrast-enhanced CT on MR-linac liver SBRT treatment plans" received the approval of the ethic Committee of Sichuan Cancer Hospital located in 55th Renmin South Road, 4th Section, 610041, Chengdu, China (Approval number SCCHEC-02-2024-078).

### Consent for publication
Even if no individual patient data were reported, consensus has been received by every patient for the elaboration of its data and for future scientific publication.

### Competing interests
The authors declare no competing interests.

### Author details
[1]College of Computer Science and Cyber Security, Chengdu University of Technology, Chengdu, China
[2]Department of Radiation Oncology, Sichuan Cancer Hospital & Institute, Affiliated Cancer Hospital of University and Electronic Science and Technology of China, Chengdu, China
[3]Sichuan Clinical Research Center for Cancer, Sichuan Cancer Center, Chengdu, China
[4]Department School of Data Science and Artificial Intelligence, Wenzhou University of Technology, Wenzhou, China
[5]Department of Gynecology and Obstetrics, West China Second University Hospital, Sichuan University, Chengdu, China

### References
1. De Ruysscher D, Faivre-Finn C, Nestle U, Hurkmans CW, Le Pechoux C, Price A, et al. European Organisation for Research and Treatment of Cancer recommendations for planning and delivery of high-dose, high-precision radiotherapy for lung cancer. J Clin Oncol. 2010;28(36):5301–10.
2. Dawson LA, Eccles C, Craig T. Individualized image guided iso-NTCP based liver cancer SBRT. Acta Oncol. 2006;45(7):856–64.
3. Shibamoto Y, Naruse A, Fukuma H, Ayakawa S, Sugie C, Tomita N. Influence of contrast materials on dose calculation in radiotherapy planning using computed tomography for tumors at various anatomical regions: a prospective study. Radiother Oncol. 2007;84(1):52–5.

4.    Xiao J, Zhang H, Gong Y, Fu Y, Tang B, Wang S, et al. Feasibility of using intra-venous contrast-enhanced computed tomography (CT) scans in lung cancer treatment planning. Radiother Oncol. 2010;96(1):73–7.
5.    Zhang J, Wang L, Xu B, Huang M, Chen Y, Li X. Influence of using a contrast-enhanced CT image as the primary image on CyberKnife Brain Radiosurgery Treatment Plans. Front Oncol. 2021; 11.
6.    Kim HJ, Chang AR, Park YK, Ye SJ. Dosimetric effect of CT contrast agent in CyberKnife treatment plans. Radiat Oncol. 2013;8:244.
7.    Woodings SJ, Bluemink JJ, de Vries JHW, Niatsetski Y, van Veelen B, Schillings J, et al. Beam characterisation of the 1.5 T MRI-linac. Phys Med Biol. 2018;63(8):085015.
8.    Lagendijk JJ, Raaymakers BW, van Vulpen M. The magnetic resonance imaging-linac system. Semin Radiat Oncol. 2014;24(3):207–9.
9.    Young T, Thwaites D, Holloway L. Assessment of electron density effects on dose calculation and optimisation accuracy for nasopharynx, for MRI only treatment planning. Australas Phys Eng Sci Med. 2018;41(4):811–20.
10.   Andreasen D, Van Leemput K, Hansen RH, Andersen JA, Edmund JM. Patch-based generation of a pseudo CT from conventional MRI sequences for MRI-only radiotherapy of the brain. Med Phys. 2015;42(4):1596–605.
11.   Raaymakers BW, Jurgenliemk-Schulz IM, Bol GH, Glitzner M, Kotte A, van Asselen B, et al. First patients treated with a 1.5 T MRI-Linac: clinical proof of concept of a high-precision, high-field MRI guided radiotherapy treatment. Phys Med Biol. 2017;62(23):L41–50.
12.   Intven MPW, de Mol van Otterloo SR, Mook S, Doornaert PAH, de Groot-van Breugel EN, Sikkes GG, et al. Online adaptive MR-guided radiotherapy for rectal cancer; feasibility of the workflow on a 1.5T MR-linac: clinical implementation and initial experience. Radiother Oncol. 2021;154:172–78.
13.   McDonald BA, Vedam S, Yang J, Wang J, Castillo P, Lee B, et al. Initial feasibility and clinical implementation of Daily MR-Guided adaptive Head and Neck Cancer Radiation Therapy on a 1.5T MR-Linac system: prospective R-IDEAL 2a/2b systematic clinical evaluation of Technical Innovation. Int J Radiat Oncol Biol Phys. 2021;109(5):1606–18.
14.   Hall WA, Straza MW, Chen X, Mickevicius N, Erickson B, Schultz C, et al. Initial clinical experience of stereotactic body Radiation Therapy (SBRT) for liver metastases, primary liver malignancy, and pancreatic cancer with 4D-MRI based online adaptation and real-time MRI monitoring using a 1.5 Tesla MR-Linac. PLoS ONE. 2020;15(8):e0236570.
15.   Mayinger M, Ludwig R, Christ SM, Dal Bello R, Ryu A, Weitkamp N, et al. Benefit of replanning in MR-guided online adaptive radiation therapy in the treatment of liver metastasis. Radiat Oncol. 2021;16(1):84.
16.   van de Lindt TN, Nowee ME, Janssen T, Schneider C, Remeijer P, van Pelt VWJ, et al. Technical feasibility and clinical evaluation of 4D-MRI guided liver SBRT on the MR-linac. Radiother Oncol. 2022;167:285–91.
17.   Tang B, Liu M, Wang B, Diao P, Li J, Feng X, et al. Improving the clinical workflow of a MR-Linac by dosimetric evaluation of synthetic CT. Front Oncol. 2022;12:920443.
18.   Okumus A, Durmus IF. Determination of Tumor size and Hounsfield Unit/Electron Density Values in three different CT scans for lung SBRT Planning. Int J Hematol Oncol. 2021;31(3):192–98.
19.   Nhila O, Talbi M, El Mansouri MH, El Katib M, Chakir EM. Evaluation of CT Acquisition Protocols Effect on Hounsfield Units and optimization of CT-RED calibration curve selection in Radiotherapy Treatment Planning systems. Mosc Univ Phys Bull. 2022;77(4):661–71.
20.   Xiao J, Li Y, Jiang Q, Sun L, Henderson F Jr, Wang Y, et al. Hepatic arterial phase and portal venous phase computed tomography for dose calculation of stereotactic body radiation therapy plans in liver cancer: a dosimetric comparison study. Radiat Oncol. 2013;8:1–7.
21.   Kamal R, Thaper D, Kumar R, Singh G, Yadav HP, Oinam AS, et al. Dosimetric impact of contrast-enhanced 4d computed tomography for stereotactic body radiation therapy of hepatocelluar carcinoma. Rep Pract Oncol Radiother. 2021;26(4):598–604.
22.   Boldrini L, Corradini S, Gani C, Henke L, Hosni A, Romano A et al. MR-guided radiotherapy for liver malignancies. Front Oncol. 2021;11:616027.
23.   Valletta R, Bonatti M, Vingiani V, Corato V, Proner B, Lombardo F et al. Feasibility of a single-phase portal venous CT protocol using bolus tracking technique and lean body weight-based contrast media dose. European Radiology. 2024; August: 1–9.
24.   Silverman PM. Multislice CT in imaging the liver. Cancer Imaging. 2003;3(2):149–54.
25.   Yu X, He L, Wang Y, Dong Y, Song Y, Yuan Z, et al. A deep learning approach for automatic tumor delineation in stereotactic radiotherapy for non-small cell lung cancer using diagnostic PET-CT and planning CT. Front Oncol. 2023;13:1235461.
26.   Stereotactic Ablative Body Radiation Therapy (SABR). A resource, version 6.1. UK SABR Consortium. 2019.
27.   Benedict SH, Yenice KM, Followill D, Galvin JM, Hinson W, Kavanagh B, et al. Stereotactic body radiation therapy: the report of AAPM Task Group 101. Med Phys. 2010;37(8):4078–101.
28.   Snyder JE, St-Aubin J, Yaddanapudi S, Boczkowski A, Dunkerley DAP, Graves SA, et al. Commissioning of a 1.5T Elekta Unity MR-linac: a single institution experience. J Appl Clin Med Phys. 2020;21(7):160–72.
29.   Wang C, Chao M, Lee L, Xing L. MRI-based treatment planning with electron density information mapped from CT images: a preliminary study. Technol Cancer Res Treat. 2008;7(5):341–47.
30.   Winkel D, Gijsbert HB, Kroon PS, Asselen BV, Hackett SS, Werensteijn-Honingh AM, et al. Adaptive radiotherapy: the Elekta Unity MR-linac concept. Clin Translational Radiation Oncol. 2019;18:54–9.
31.   Feng X, Tang B, Yao X, Liu M, Liao X, Yuan K et al. Effectiveness of bladder filling control during online MR-guided adaptive radiotherapy for rectal cancer. Radiat Oncol. 2023; 18 (1).
32.   Paddick I. A simple scoring ratio to index the conformity of radiosurgical treatment plans. J Neurosurg. 2000;93(supplement3):219–22.
33.   Paddick I, Lippitz B. A simple dose gradient measurement tool to complement the conformity index. J Neurosurg. 2006;105(Suppl):194–201.
34.   Scott JA. Photon, Electron, Proton and Neutron Interaction Data for Body Tissues ICRU Report 46. International Commission on Radiation Units and Measurements. 1992.
35.   ICRP. ICRP publication 110: adult reference computational phantoms. Ann ICRP. 2009; 39 (2).
36.   Seco J, Sharp GC, Wu Z, Gierga D, Buettner F, Paganetti H. Dosimetric impact of motion in free-breathing and gated lung radiotherapy: a 4D Monte Carlo study of intrafraction and interfraction effects. Med Phys. 2008;35(1):356–66.
37.   Guerreiro F, Burgos N, Dunlop A, Wong K, Petkar I, Nutting C, et al. Evaluation of a multi-atlas CT synthesis approach for MRI-only radiotherapy treatment planning. Physica Med. 2017;35:7–17.
38.   Moorrees J, Bezak E. Four dimensional CT imaging: a review of current technologies and modalities. Australasian Phys Eng Sci Med. 2012;35:9–23.
39.   Koide Y, Shimizu H, Wakabayashi K, Kitagawa T, Aoyama T, Miyauchi R, et al. Synthetic breath-hold CT generation from free-breathing CT: a novel deep learning approach to predict cardiac dose reduction in deep-inspiration breath-hold radiotherapy. J Radiation Res. 2021;62(6):1065–1075.

## Publisher's note